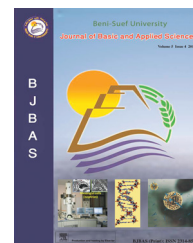


Available online at [www.sciencedirect.com](http://www.sciencedirect.com)

journal homepage: [www.elsevier.com/locate/bjbas](http://www.elsevier.com/locate/bjbas)

## Full Length Article

# Removal of hexavalent chromium from aqueous solutions by adsorption on modified groundnut hull

Samson O. Owalude\*, Adedibu C. Tella

Department of Chemistry, University of Ilorin, P.M.B. 1515, Ilorin, Nigeria

### ARTICLE INFO

#### Article history:

Received 18 August 2015

Received in revised form 4

November 2016

Accepted 7 November 2016

Available online 10 November 2016

#### Keywords:

Adsorption

Groundnut hull

Hexavalent chromium

Waste water

Adsorption kinetics

### ABSTRACT

There is an emerging serious threat to the environment from indiscriminate release of heavy metals into the wastewaters and soil from human industrial practices. In this study therefore, the uptake of hexavalent chromium, being among the major pollutants from our industries, by modified and unmodified groundnut hull was investigated. The effects of different conditions of contact time, adsorbate concentration, solution pH, and temperature on sorption process were studied. The adsorbent materials were characterized by Fourier Transform Infrared Spectroscopy (FT-IR). Analysis of the surface morphology by Scanning Electron Microscopy (SEM) revealed a change in morphology upon chromium adsorption. The adsorption process of Cr(VI) ions onto both the unmodified groundnut hull (UGS) and the modified groundnut hull (MGS) is in good agreement with the Langmuir adsorption isotherm and follows the pseudo-second-order kinetic model. According to the equilibrium studies, chromium(VI) ions are better adsorbed by modified groundnut hull.

© 2016 Beni-Suef University. Production and hosting by Elsevier B.V. This is an open access article under the CC BY-NC-ND license (<http://creativecommons.org/licenses/by-nc-nd/4.0/>).

## 1. Introduction

The release of heavy metals into wastewater through human and industrial activities has become a major problem both to humans and aquatic lives (Wang et al., 2011). Chromium as a heavy metal is ranked among the top sixteen toxic pollutants that have harmful effects on human health (Gardea-Torresday et al., 2000). High chromium dosage has been reported to cause damage to human kidney and the liver (Mungasavalli et al., 2007); and at low concentration it causes skin irritation and

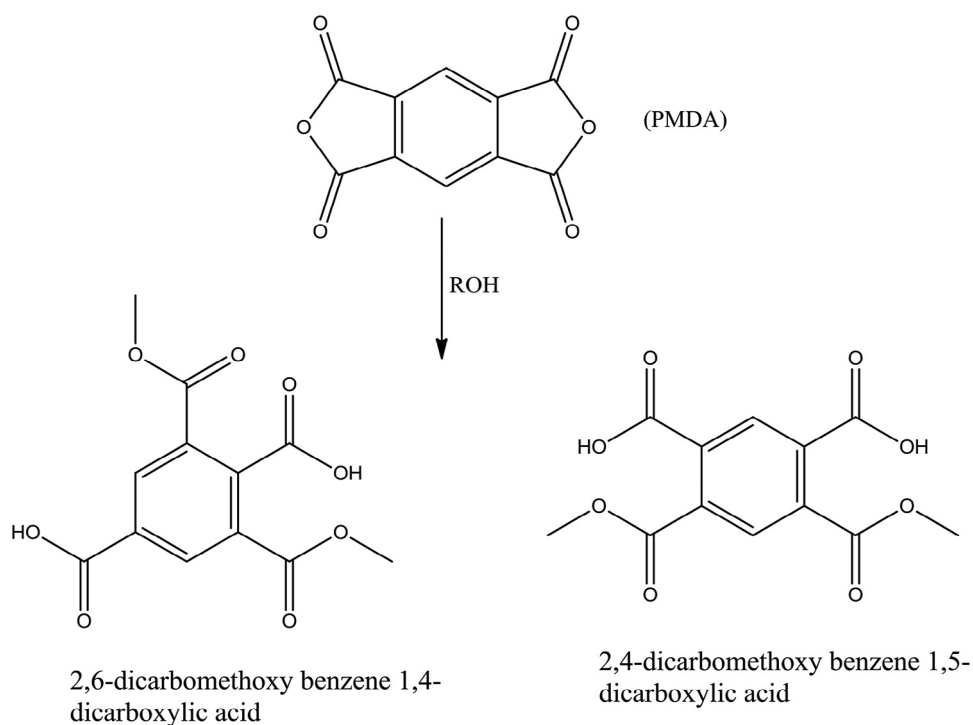
ulceration (Karthikeyan et al., 2005). Exposure to high chromium concentration also causes cancer in the digestive tract and lungs (Ofudje et al., 2014). Therefore, indiscriminate discharge of heavy metals in general into aquatic bodies and sources of potable water has to be regulated through enactment of legal standards and strict environmental control mechanism (Garg et al., 2004). For the removal of dissolved heavy metal ions, several techniques such as solvent extraction, ion exchange, membrane process, electrodialysis, precipitation, phytoextraction, ultra filtration, reverse osmosis and adsorption have been tested. These methods except adsorption are non-economical with

\* Corresponding author. Department of Chemistry, University of Ilorin, P.M.B. 1515, Ilorin, Nigeria.

E-mail addresses: [owalude1412@yahoo.com](mailto:owalude1412@yahoo.com); [owalude@unilorin.edu.ng](mailto:owalude@unilorin.edu.ng) (S.O. Owalude).

<http://dx.doi.org/10.1016/j.bjbas.2016.11.005>

2314-8535/© 2016 Beni-Suef University. Production and hosting by Elsevier B.V. This is an open access article under the CC BY-NC-ND license (<http://creativecommons.org/licenses/by-nc-nd/4.0/>).



**Scheme 1 – Ring opening reactions of PMDA in solutions.**

disadvantages such as incomplete metal removal, high reagent cost, energy requirements and generation of toxic sludge or other waste products that require further disposal or treatment. The adsorption technique remains the most preferred method because of its efficiency and low cost (Li et al., 2007).

Many investigations have been carried out on the effective removal of heavy metals from solution using natural adsorbents derived from agricultural wastes (Singh et al., 2006; Sarin and Pant, 2006; Sun and Shi, 1998, etc.). The present study is therefore carried out to investigate the possible use of groundnut shell, an agricultural waste material, for the removal of chromium ions from aqueous solution.

Nigeria in the past was renowned for the production of groundnut which then competed favorably with cocoa as major cash crops. In fact, these two crops constituted the highest percentage of Nigeria export earnings before the discovery of petroleum in the 1960s. With the new national policy on agriculture of the government of the Federal Republic of Nigeria, the famous groundnut pyramids (the systematic way of arranging groundnuts in a large building, constructed in form of square or triangle which is specifically for the purpose of storing groundnuts) is expected back. The performance of groundnut shells was therefore investigated for the removal of hexavalent chromium from aqueous solution. The material is readily available, biodegradable, cost-free and easily found in large quantity in the northern states of Nigeria.

Pyromellitic dianhydride (PMDA) has the capacity to undergo ring opening reactions in solutions to produce 2,6-dicarbomethoxy benzene 1,4-dicarboxylic acid or its isomer 2,4-dicarbomethoxy benzene 1,5-dicarboxylic acid as shown in Scheme 1. Several first row transition metal dicarboxylate complexes have been prepared through this reaction (Baruah et al., 2007). Therefore, when attached to the surface of adsorbents,

PMDA introduces a large number of carboxyl groups onto its surface resulting into a material with an enhanced ability to adsorb cationic substances. Literature reports have shown that the adsorption capacities of several adsorbents have been significantly increased on modification with PMDA (He et al., 2013; Yu et al., 2012, 2015).

We have therefore investigated the adsorptive capacity of PMDA-modified groundnut hulls for the removal of hexavalent chromium from aqueous solutions. The effects of some parameters such as, contact time, solution pH, adsorbent dose and initial chromium ions concentrations on the performance of the adsorbent on the sorption process were investigated. Scanning electron microscopy (SEM) and Fourier transform infrared spectroscopy (FTIR) were used to analyze the possible mechanism of the adsorption process. The equilibrium data were analyzed using Langmuir and Freundlich isotherm models.

## 2. Experimental

### 2.1. Materials and methods

All chemicals used in this work were of analytical grade and the aqueous solutions were prepared using deionized double distilled water. The morphology of the surface of the groundnut hulls were studied by Scanning Electron Microscope (SEM). The acceleration voltage (Acc.V) was 15.0 kV, and the spot size (SE) was 200  $\mu\text{m}$ . The Fourier Transform Infrared Spectroscopy (FT-IR) of both the UGS and MGS were recorded on NEXUS 670 Spectrophotometer. Solutions of chromium were prepared using potassium dichromate. The groundnut hulls were obtained from a local groundnut milling center at Ipata market here in Ilorin,

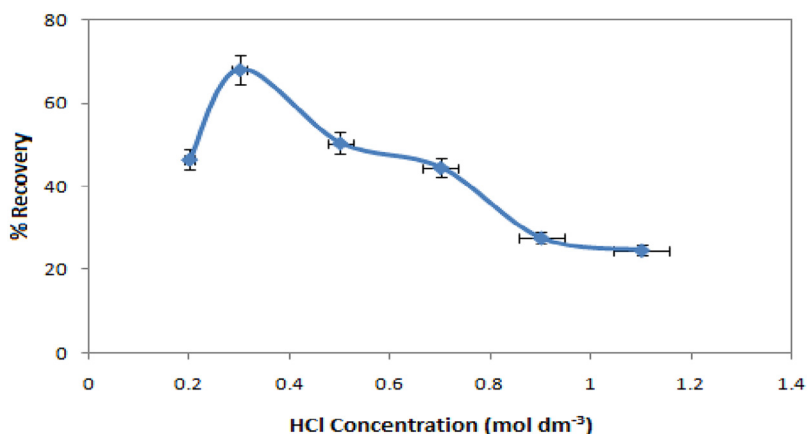


Fig. 1 – The Recovery of Cr(VI) ions from MGS after adsorption.

Nigeria. The hulls were washed severally with clean water, and then boiled for 6 hours in order to remove dirt and colored compounds. On cooling, the shells were rinsed with distilled water. The washing was continued until the filtrate become colorless. The resulting material was dried in the oven maintained at 80 °C for 24 hours and thereafter ground to powder; the powder was sieved by a size fraction of 200–300 μm. This unmodified sample is labeled UGS. Portions of the groundnut hull were then modified with pyromellitic dianhydride (PMDA) using a procedure described in the literature (Yu et al., 2015) and labeled MGS. The dried samples of both UGS and MGS were stored in a desiccator at room temperature.

## 2.2. Batch adsorption study

The sorption experiments were carried out under different conditions of pH, contact time, temperature, and sorbate concentration. Batch adsorption experiments were performed by contacting appropriate amount of either UGS or MGS with 100 mL of an aqueous hexavalent chromium solution with different initial concentrations at different solution pH. Experiments were usually carried out for 120 min at 28 °C in 250 mL stoppered conical flasks, which were placed in an HY-2 orbital shaker working with a constant agitation speed of 125 rpm. The mixture was stirred continuously to make provision for better mass transfer with high interfacial surface area. A 1000 ppm hexavalent chromium stock solution was prepared by dissolving 5.66 g of potassium dichromate in 1 L of water and different initial concentrations were obtained by subsequent dilution of this stock. The effect of Cr(VI) concentration was then carried out using  $6.0 \times 10^{-5}$  M,  $1.2 \times 10^{-4}$  M,  $1.8 \times 10^{-4}$  M,  $2.5 \times 10^{-4}$  M,  $3.20 \times 10^{-4}$  M and  $4.5 \times 10^{-4}$  M of Cr(VI) solution on equal amount of adsorbent. The effect of the adsorbent dosage on the equilibrium adsorption of Cr(VI) on both UGS and MGS were studied at different adsorbent dosages between 10–50 mg. The adsorption kinetics was studied by analyzing the adsorptive uptake of Cr(VI) ions from aqueous solutions at different time intervals. The effect of pH was studied at pH between 1 and 8 by the addition of appropriate amount of  $0.1 \text{ mol dm}^{-3}$  HCl or  $0.1 \text{ mol dm}^{-3}$  NaOH solutions. The batch experiments were also carried out at different temperatures between 283 and 313 K. After adsorption, the adsorbent and the supernatants were separated centrifuga-

tion at 1500 rpm for 10 min. The supernatants were analyzed for residual Cr(VI) ions using a UV-visible spectrophotometer, by monitoring the absorbance changes at  $\lambda_{\text{max}}$  of 370 nm.

## 2.3. Chromium analysis

The amount of hexavalent chromium adsorbed per g of the adsorbent was estimated using the formula:

$$Q_e = \frac{(C_o - C_e)V}{w} \quad (1)$$

Where  $C_o$  and  $C_e$  are the initial and equilibrium liquid phase concentrations of the Cr(VI) ions in  $\text{mg L}^{-1}$  respectively,  $V$  is the volume of the solution in L and  $w$  is the amount of adsorbent used in g.

## 2.4. Desorption experiment

Reusability of the adsorbent was tested by regenerating the spent adsorbent following a modified literature procedure (Dehghani et al., 2016). 0.3 g of the used adsorbent was contacted with distilled water (DW), 0.01, 0.1, 1.0 and 1.20 M HCl solutions. The results show that the highest percentage (68%) of the adsorbed Cr(VI) was desorbed from MGS when contacted with 0.3 M HCl (Fig. 1). Recovery of Cr(VI) from UGS followed the same pattern as for MGS except that the highest percentage removal of 79.62% was obtained at 0.3 M HCl. These results indicate that substantial amount of Cr(VI) ions can be recovered from the spent adsorbent making it reusable. After the desorption experiments, the adsorbents were collected from the solution by filtration, washed several times with distilled water, dried in the oven at 80 °C for 24 h and then reused for Cr(VI) removal. The recovered adsorbent is reusable over at least three cycles.

## 3. Results and discussion

### 3.1. Characterization of the adsorbent

#### 3.1.1. SEM studies

The Scanning Electron Microscope (SEM) images shown in Fig. 2 revealed the nature of the morphology of the modified

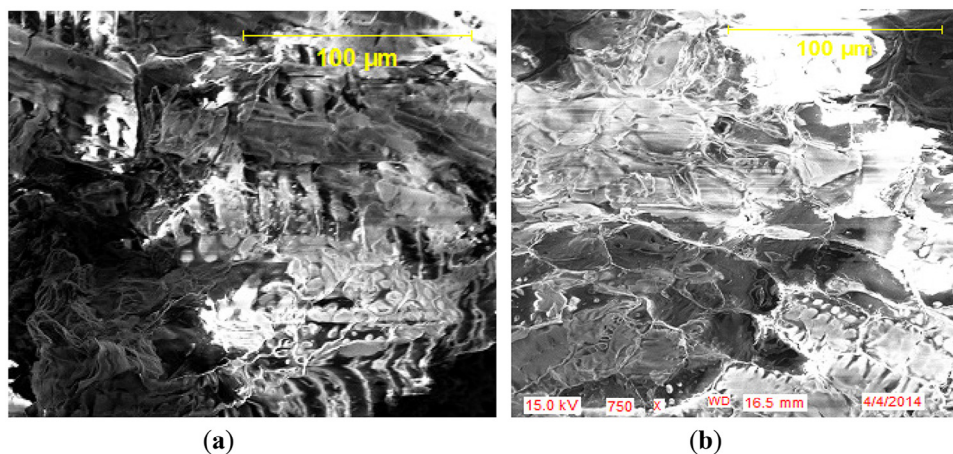


**Fig. 2 – SEM images of the modified groundnut Shell (a) = MGS before adsorption of chromium(VI) (b) = MGS after adsorption of chromium(VI).**

adsorbent before and after adsorption. Fig. 2a shows unoccupied pores on the adsorbent before adsorption while Fig. 2b shows the morphology of the adsorbent after the loading of Cr(VI) ions. As seen in Fig. 2b, the outer pores are covered by Cr(VI) ions and the pores are no longer visible. This is an evidence for the adsorption of Cr metal ions on the surface of the adsorbent material.

### 3.1.2. Infra-red spectroscopy

Fig. 3a depicts the FT-IR spectrum of the unmodified groundnut shell. The broad band in the region around  $3425\text{ cm}^{-1}$  is assigned to the surface hydroxyl groups of bonded carboxylic acid (Han et al., 2006). The O–H stretching vibrations occurred within a broad range of frequencies indicating the presence of free hydroxyl groups and bonded O–H bands of carboxylic acid (Han et al., 2006). The asymmetric C–H stretching of surface methyl groups usually present on the lignin structure is observed at  $2918\text{ cm}^{-1}$ . The characteristic peaks due to the C–O group in carboxylic and alcoholic groups were present at  $1053$  and  $1033\text{ cm}^{-1}$  (Krishnani et al., 2008). The ionization of both the carboxylic acid and hydroxyl functional groups present in the structure of the adsorbent can be achieved by deprotonation making it to interact with metals easily and therefore may be the major biosorption sites for the removal of hexavalent chromium ions from solutions (Han et al., 2006). The -OH, -NH, carbonyl and carboxylic groups have been reported as very important sorption sites for metal ions (Kalaivani et al., 2014). A new peak due to the carbonyl group stretching of PDMA is observed as a sharp peak at  $1734\text{ cm}^{-1}$  in the FT-IR spectrum of the modified groundnut hull shown in Fig. 3b. The peaks at  $1508\text{ cm}^{-1}$  are associated with aromatic ring stretching while those observed at  $1071$  and  $1024\text{ cm}^{-1}$  are due to C–H and C–O bonds. The FT-IR spectrum of the groundnut hull obtained after adsorption of chromium(VI) ions is shown in Fig. 3c, and when compared to Fig. 3b, a broadening of the -OH peak at around  $3400\text{ cm}^{-1}$  and carbonyl group peak at  $1633\text{ cm}^{-1}$  was observed. This indicates the involvement of hydroxyl and carbonyl groups in the adsorption of chromium(VI).

### 3.2. Effect of various adsorption parameters

The removal efficiencies of the two adsorbents were investigated and compared based on the following results. The adsorption capacity  $Q_e$  is calculated from the expression in equation 1 while the percentage chromium(VI) removal is obtained using equation 2.

$$\% \text{ removal} = \frac{(C_o - C_e)}{C_o} \times 100 \quad (2)$$

Where  $C_o$  = initial adsorbate concentration (mg/L);  $C_e$  = final equilibrium adsorbate concentration (mg/L).

#### 3.2.1. Effect of adsorbent dosage

It can be observed from Fig. 4 that the adsorption of hexavalent chromium increased from 52 to 88% and 72 to 98% for UGS and MGS respectively with increase in adsorbent dosage for both adsorbents from 5 to 40 mg. This is attributed to increased adsorbent surface area and availability for more adsorption sites (Rao et al., 2002; Umoren et al., 2013). The modified groundnut shell is seen to be more effective.

#### 3.2.2. Effect of Cr(VI) concentration

The performance efficiency of both the UGS and MGS were studied at different initial hexavalent chromium concentrations while maintaining constant the other parameters. The efficiency of the adsorbent increases as the concentration of Cr(VI) ions increases up to 12.5 mg/L when the efficiency remained almost constant up to 18 mg/L and starts to decrease thereafter for MGS (Fig. 5). The same trend was observed for UGS except that maximum efficiency was attained at 8.3 mg/L. This is attributed to the fact that the available surface area of the adsorbents become smaller as Cr(VI) molecules got adsorbed on to the adsorbent surface (Banat et al., 2000). When the Cr(VI) concentration is sufficiently large, the adsorbent's surface got occupied and the efficiency starts to decrease and the molecules desorbed from the adsorbent's surface. The modified groundnut hull in general adsorbs better than the unmodified groundnut shell.

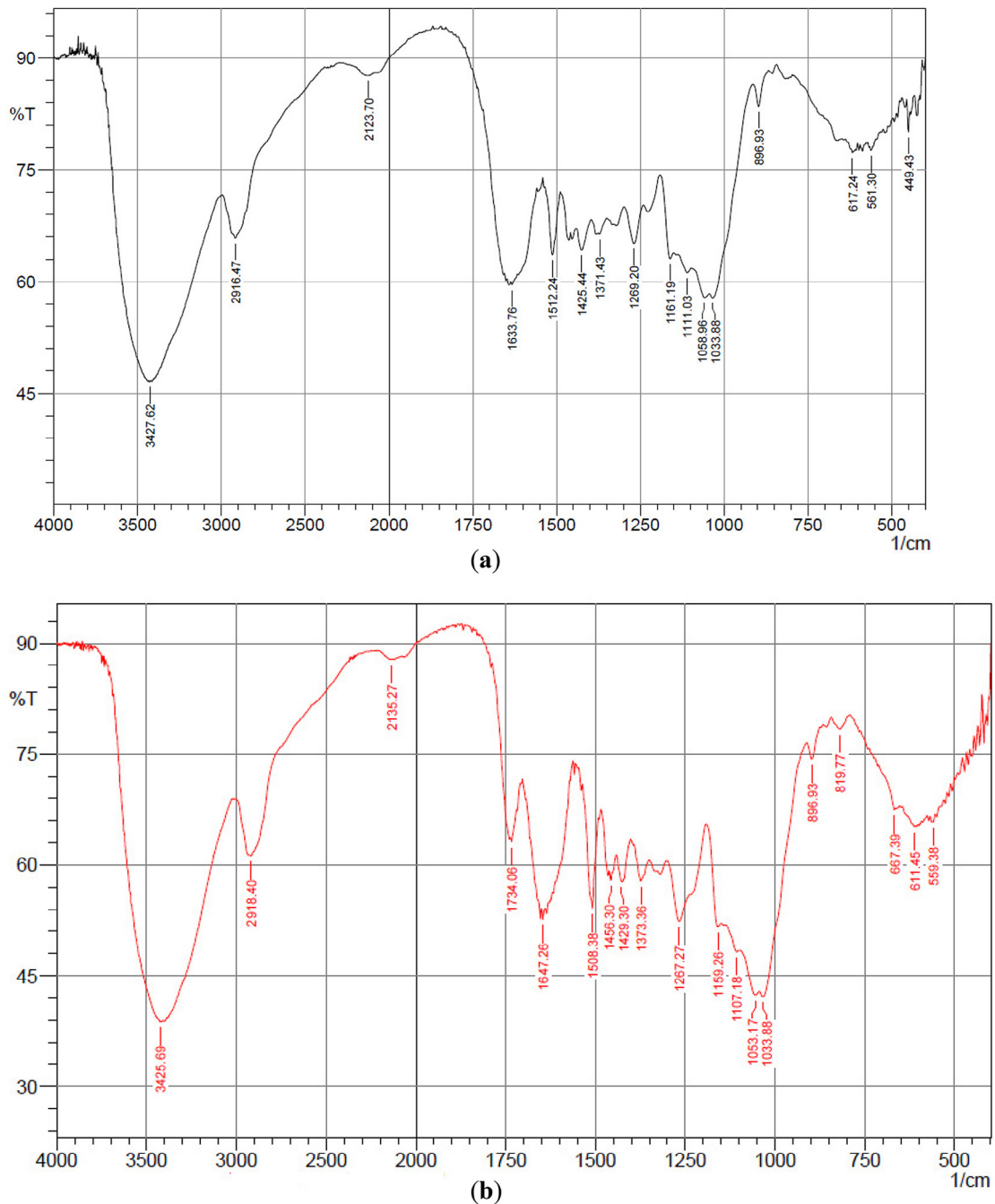


Fig. 3 – FTIR spectra of (a) unmodified groundnut shell and (b) modified groundnut shell.

### 3.2.3. Effect of pH

The effect of pH on the adsorption process was investigated by undertaking the batch adsorption procedure at different hydrogen ion concentrations while maintaining constant the other parameters. The pH of the adsorption medium was varied between 1 and 8, the modified adsorbent (MGS) gave the highest performance of 96% at the pH = 2 while the unmodified adsorbent (UGS) at the same pH gave highest performance of 82% (Fig. 6). The maximum performance was therefore obtained at pH 2 and hence all the other experiments were performed at this pH value. In aqueous solutions, Cr(VI) exist in several stable forms such as  $\text{CrO}_4^{2-}$ ,  $\text{HCrO}_4^-$ , and  $\text{Cr}_2\text{O}_7^{2-}$  (Alfa-Sika et al., 2010).

At the pH of maximum adsorption in this study (pH 2), the dominant species has been reported to be  $\text{HCrO}_4^-$  (Cimino et al., 2000). The chemical nature of the functional groups on both the modified and unmodified groundnut hulls can be altered by changes in the pH of the adsorption medium and by extension the metal sorption capacity of the adsorbents (Yu et al., 2015). Competition for the same sorption sites with metal ions by hydrogen ions at low pH values has been reported (Fourest and Roux, 1992; Yan et al., 2010). It is therefore believed that the adsorption sites on the surface of both the UGS and MGS are occupied by hydrogen ions ( $\text{H}^+$ ) thereby making the surface positively charged. This will allow the approaching negatively charged  $\text{HCrO}_4^-$  ions

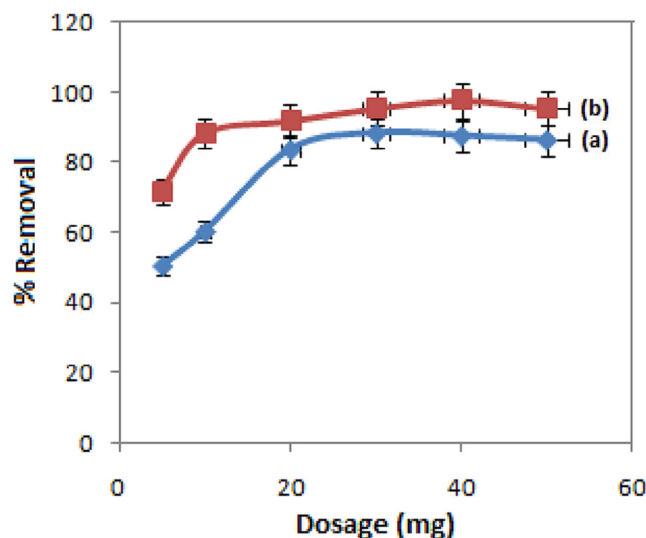


Fig. 4 – Effect of adsorbent dose on Cr(VI) ions removal from aqueous solution using groundnut shell adsorbent at 28 °C, pH = 2, time = 60 mins and [Cr(VI)] = 13 mg/L. (a) = UGS, (b) = MGS.

oto easy access to the binding sites on the adsorbents so that greater metal ions can be adsorbed due to electric attraction with hydrogen ions on the adsorbent.

#### 3.2.4. Effect of temperature

The effect of temperature for the removal of Cr(VI) ions by both the UGS and MGS were studied at different temperatures between 30 and 70 °C as shown in Fig. 7. Maximum adsorption capacity was obtained at 30 °C for both adsorbents at pH of 2. The adsorption capacity decreased with increase in temperature suggesting that the adsorption process was exothermic (Vidhyadevi et al., 2014). As observed in Fig. 4, the MGS gave better performance adsorption than the UGS.

These results also indicate that during the adsorption process, no permanent chemical bonds are formed (Kalaivani et al., 2014).

#### 3.2.5. Effect of contact time

The effect of contact time on Cr(VI) adsorption on UGS and MGS was carried out at room temperature. The plots of the percentage removal of hexavalent chromium vs contact time for adsorbents are shown in Fig. 8. There was very rapid adsorption at the initial period up to 30 min for both adsorbents (UGS and MGS) and above 30 min the increase in adsorption rate were not well pronounced. This is attributed to the larger surface area of the UGS and MGS being available at the beginning for the adsorption of hexavalent chromium ions. The adsorption process attained equilibrium in 80 min with MGS and in 60 min with UGS, after which the amount of Cr(VI) ions adsorbed from solutions remains unchanged. This has been attributed to the active sites present in the adsorbents' surfaces being saturated by the Cr(VI) molecules (Kannan et al.,

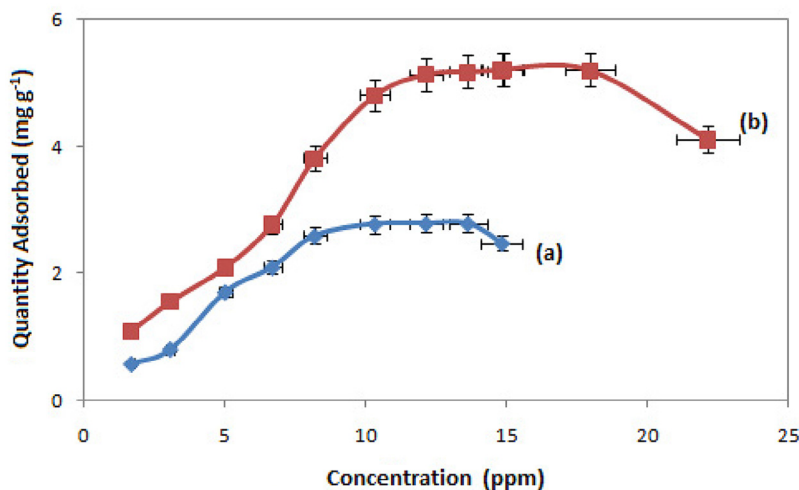


Fig. 5 – Effect of Cr(VI) concentration on the adsorption rate from aqueous solution using groundnut shell adsorbent at 28 °C, pH = 2, time = 60 mins and adsorbent dose = 30 mg (a) = UGS, (b) = MGS.

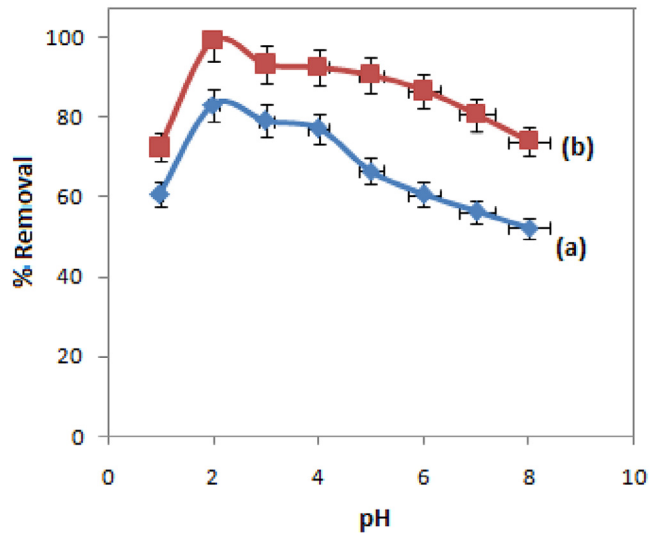


Fig. 6 – Effect of pH on the adsorption of Cr(VI) ions from aqueous solution using groundnut shell adsorbent at 28 °C, time = 60 mins, adsorbent dose and [Cr(VI)] = 13 mg/L. (a) = UGS, (b) = MGS.

2013). Even within 20 mins, the MGS adsorbent showed better removal of Cr(VI) ions from solution than the UGS adsorbent.

### 3.3. Adsorption isotherm studies

For solid-liquid adsorption system, the adsorption behavior can well be described by adsorption isotherm model (Tella et al., 2014). The adsorption isotherm can indicate the distribution of adsorbate molecules between the solid phase and the liquid phase at equilibrium. Equilibrium is said to be established when the concentration of adsorbate in bulk solution is in dynamic balance with that on the liquid adsorbate interface (Aksu, 2002). It is significant to understand the adsorption behavior in order to describe adsorption process using appropriate adsorption isotherm model. Therefore, the distribution of Cr(VI) ions between the adsorbent and solution was determined by Langmuir and Freundlich adsorption isotherms by fitting the

equilibrium adsorption data into their respective isotherm equations (Freundlich, 1906; Langmuir, 1918).

#### 3.3.1. Langmuir adsorption isotherm

The equilibrium adsorption data for the concentrations of Cr(VI) ions was fitted into the linear form of Langmuir's isotherm equation (3) to determine the distribution of Cr(VI) ions between the adsorbent and solution:

$$\frac{C_e}{Q_e} = \frac{1}{Q_m K_L} + \frac{C_e}{Q_e} \quad (3)$$

Where  $C_e$  is the equilibrium concentration of the chromium ions in solution ( $\text{mg L}^{-1}$ ),  $Q_e$  is the equilibrium concentration of Cr(VI) ions on the groundnut shell adsorbent ( $\text{mg g}^{-1}$ ),  $Q_m$  and  $K_L$  are Langmuir constants related to

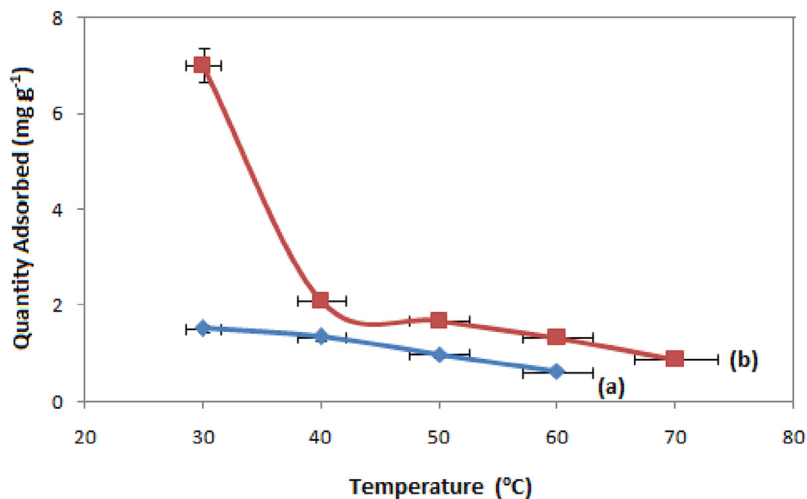


Fig. 7 – Effect of Temperature on the adsorption of Cr(VI) from aqueous solution using groundnut shell adsorbent at pH = 2, time = 60 mins, adsorbent dose = 2 g and [Cr(VI)] = 13 mg/L. (a) = UGS, (b) = MGS.

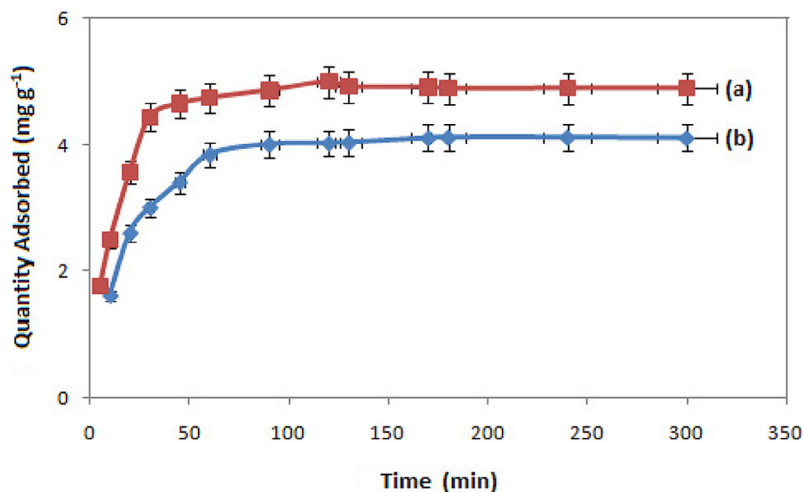


Fig. 8 – Effect of contact time on the adsorption of Cr(VI) from aqueous solution using groundnut shell adsorbent at 28 °C, pH = 2, time = 300 mins, adsorbent dose = 2 g and [Cr(VI)] = 13 mg/L. (a) = UGS, (b) = MGS.

sorption capacity and the rate of adsorption respectively. Maximum adsorption capacity ( $Q_m$ ) is the monolayer capacity of the adsorbent ( $\text{mg g}^{-1}$ ) and  $K_L$  is the Langmuir adsorption constant. A plot of  $C_e/Q_e$  against  $C_e$  over the entire concentration range is a straight line with a slope of  $1/Q_m$  and the intercept of  $1/Q_m K_L$  (Fig. 9). The correlation coefficient ( $R^2$ ) values reported in Table 1 for both UGS and MGS are very close to 1 indicating that the adsorption follows the Langmuir adsorption isotherm for the two adsorbents. The maximum monolayer

adsorption capacity of UGS is 90 and for MGS is 131, this clearly indicates that MGS has better affinity for Cr(VI) ions than UGS.

The quality of Langmuir isotherm can be determined by the magnitude of a dimensionless constant  $R_L$  known as the separation factor expressed in equation 4 (Tang et al., 2013).

$$R_L = \frac{1}{1 + K_L C_0} \tag{4}$$

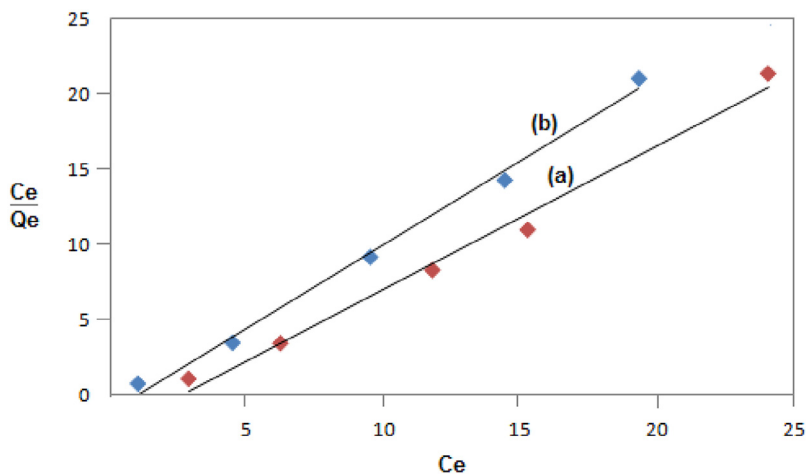


Fig. 9 – Langmuir isotherm plots for the adsorption of Cr(VI) removal from aqueous solution groundnut shell adsorbent at 28 °C, pH = 2, time = 60 mins, adsorbent dose = 2 g and [Cr(VI)] = 13 mg L<sup>-1</sup>. (a) = UGS, (b) = MGS.

Table 1 – Langmuir and Freundlich adsorption isotherm parameters.

| S/No. | Langmuir isotherm |       |       | Freundlich isotherm |       |       |
|-------|-------------------|-------|-------|---------------------|-------|-------|
|       | Parameters        | UGS   | MGS   | Parameters          | UGS   | MGS   |
| 1     | $Q_{max}$ (mg/g)  | 90    | 131   | $1/n$               | 0.482 | 0.253 |
| 2     | $K_L$             | 1.030 | 2.170 | $K_F$               | 0.885 | 1.203 |
| 3     | $R^2$             | 0.988 | 0.993 | $R^2$               | 0.918 | 0.979 |
| 4     | $R_L$             | 0.31  | 0.17  |                     |       |       |



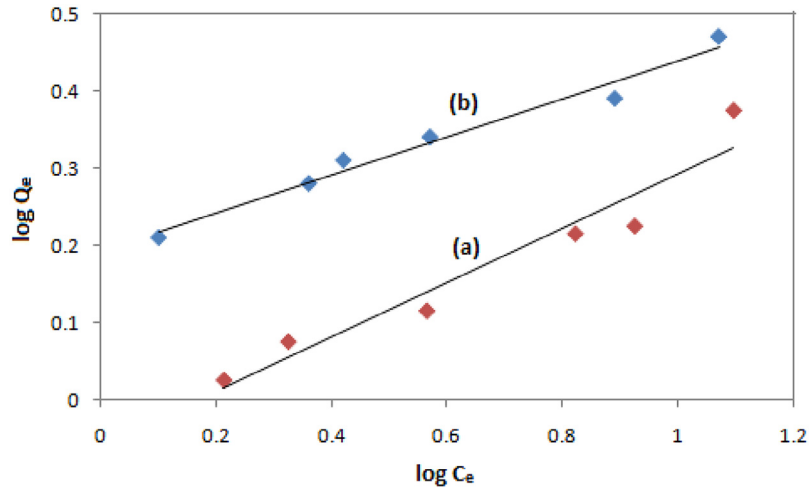


Fig. 10 – Freundlich isotherm plots for the adsorption of Cr(VI) removal from aqueous solution using groundnut shell adsorbent at 28 °C, pH = 2, time = 60 mins, adsorbent dose = 2 g and [Cr (VI)] = 13 mg L<sup>-1</sup>. (a) = UGS, (b) = MGS.

where  $C_0$  is the initial concentration of the Cr(VI) ions in mg L<sup>-1</sup> and  $K_L$  is the Langmuir constant described earlier. The adsorption process is favorable within the range  $0 < R_L < 1$ , unfavorable when  $R_L > 1$ , becomes linear when  $R_L = 1$ , and the process is irreversible when  $R_L = 0$ . The value of  $R_L$  from Table 1 is 0.31 for UGS and 0.17 for MGS; hence the adsorption process is favorable. The  $R_L$  values for both the UGS and MGS in this study are relatively low suggesting a strong interaction between the Cr(VI) molecules and the adsorbents (Sharma and Forster, 1994).

### 3.3.2. Freundlich adsorption isotherm

Equation (5) represents the linear form of the Freundlich adsorption model equation:

$$\log_e Q_e = \log_e K_f + \frac{1}{n} \log_e C_e \quad (5)$$

where  $Q_e$  is the amount of Cr(VI) ions adsorbed at equilibrium per gram of the adsorbent (mg g<sup>-1</sup>),  $C_e$  is the equilibrium concentration of the Cr(VI) ions in the solution (mg L<sup>-1</sup>), and  $K_f$  and  $n$  are the Freundlich adsorption model constants related to the adsorption capacity and adsorption intensity respectively. Using equation (5),  $\log_e Q_e$  was plotted against  $\log_e C_e$  and a straight line obtained (Fig. 10) gave the intercept of  $\log K_f$  and the slope of  $1/n$ . The numerical value of  $1/n$  reported in Table 1 is less than 1 and also positive for the two adsorbents indicating a favorable adsorption process (Kannan et al., 2013). The higher positive

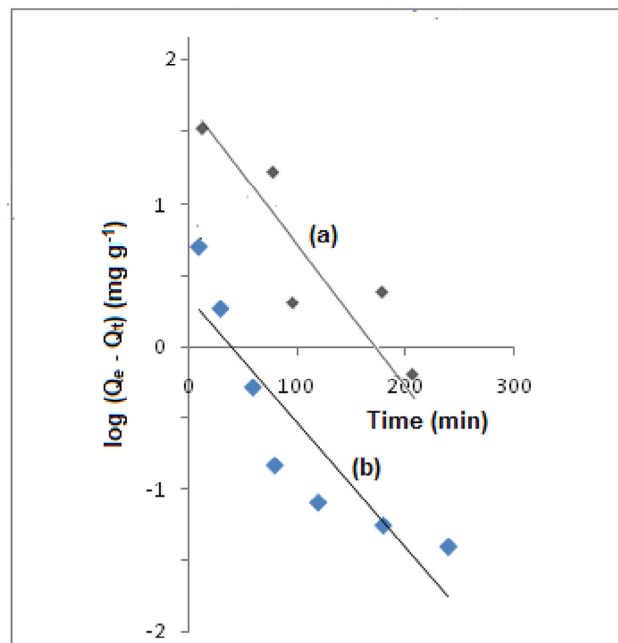


Fig. 11 – Pseudo-first-order plots for the adsorption of Cr(VI) removal from aqueous solution using groundnut shell adsorbent at 28 °C, pH = 2, time = 60 mins, adsorbent dose = 2 g and [Cr(VI)] = 13 mg L<sup>-1</sup>. (a) = UGS, (b) = MGS.

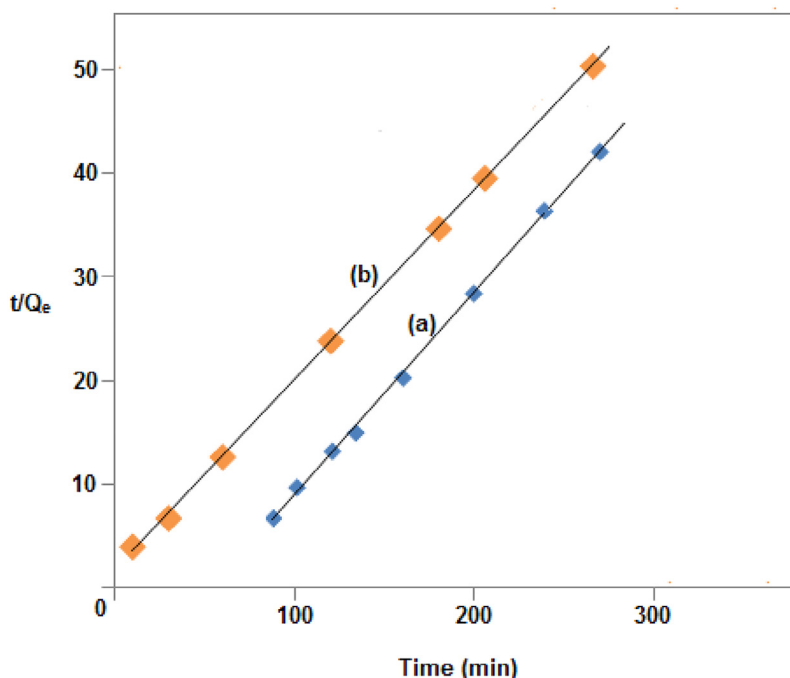


Fig. 12 – Pseudo-second-order plots for the adsorption of Cr(VI) ions removal from aqueous solution using groundnut shell adsorbent at 28 °C, pH = 2, time = 60 mins, adsorbent dose = 2 g and [Cr(VI)] = 13 mg L<sup>-1</sup>. (a) = UGS, (b) = MGS.

value of  $n$  for MGS shows that the adsorption of Cr(VI) ions onto MGS is more favorable than onto UGS. This isotherm also predicted a multilayer adsorption of the Cr(VI) ions on the surface of both the UGS and MGS (Hasany et al., 2002).

### 3.4. Adsorption kinetics

The experimental data on the effect of contact time were fitted into the pseudo-first-order and the pseudo-second-order rate equations in order to analyze the kinetics of the process of adsorption of Cr(VI) ions on both the UGS and MGS. The linear form of Lagergren's equation for pseudo-first-order adsorption kinetics is expressed as (Gupta and Bhattacharyya, 2011):

$$\ln(Q_e - Q_t) = \ln Q_e - k_1 t \quad (6)$$

where  $Q_e$  and  $Q_t$  (mg g<sup>-1</sup>) represent the amounts of Cr(VI) ions adsorbed per unit weight of the adsorbents at equilibrium and time  $t$  (min), respectively, and  $k_1$  (min<sup>-1</sup>) is the rate constant of pseudo-first-order kinetic model for the adsorption process. The values of  $k_1$  were calculated from the slope of the plots of  $\ln(Q_e - Q_t)$  versus  $t$  for both the UGS and MGS

(Fig. 11). The pseudo-second-order kinetics of adsorption of metal ions, dyes and organic substances from aqueous solutions has been successfully described by Ho's equation (Ho and McKay, 1999):

$$\frac{t}{Q_e} = \frac{t}{Q_e} + \frac{1}{k_2 Q_e^2} \quad (7)$$

Where  $k_2$  (g mg<sup>-1</sup> min<sup>-1</sup>) is the rate constant for pseudo-second-order adsorption. The plots of  $t/Q_e$  versus  $t$  gave straight lines for both adsorbents (Fig. 12). The values of  $k_2$  and  $Q_e$  were obtained from the intercepts and slopes of these straight lines as recorded in Table 2. The adsorption kinetics data fitted very well into the pseudo-second-order adsorption kinetic model with  $R^2$  value of 0.9992 for MGS and 0.9986 for the UGS compared to the corresponding  $R^2$  values of 0.8935 and 0.8091 for the pseudo-first-order kinetic model. The poor linearity of the Lagergren pseudo-first-order plots observed for the Cr(VI) ions in the present study gave an indication that the adsorption process did not follow a first-order kinetics but rather adhered more to the pseudo-second-order kinetics for both the UGS and MGS. In comparison, the MGS gave better adsorption kinetics parameters than that of the UGS.

Table 2 – Adsorption kinetics parameters.

| S/No. | Pseudo-first-order         |       |       | Pseudo-second-order                           |       |       |
|-------|----------------------------|-------|-------|---|-------|-------|
|       | Parameters                 | UGS   | MGS   | Parameters                                    | UGS   | MGS   |
| 1     | $Q_e$ (mg/g)               | 1.416 | 3.490 | $Q_e$ (mg/g)                                  | 3.143 | 5.435 |
| 2     | $k_1$ (min <sup>-1</sup> ) | 0.009 | 0.032 | $k_2$ (g mg <sup>-1</sup> min <sup>-1</sup> ) | 0.018 | 0.020 |
| 3     | $R^2$                      | 0.809 | 0.894 | $R^2$   | 0.998 | 0.999 |

**Table 3 – Comparison of adsorption capacities of MGS with other adsorbents for Cr(VI).**

| S/No | Adsorbent   | $Q_{max}$ (mg/g) | pH | Ref.                  |
|------|---|------------------|----|-----------------------|
| 1    | Rice husk carbon                                      | 47.61            | 2  | Khan et al., 2016     |
| 2    | Treated waste newspaper                               | 59.88            | 3  | Dehghani et al., 2016 |
| 3    | Plantain waste  | 16.10            |    |                       |
| 4    | Peels of pea ( <i>Pisum sativum</i> ) pod             | 4.33             | 2  | Sharma et al., 2016   |
| 5    | Tea ( <i>Camellia sinensis</i> ) waste                | 7.29             | 2  | „                     |
| 6    | Banana ( <i>Musa lacatan</i> ) waste                  | 10.0             | 2  | „                     |
| 7    | Chitosan-coated fly ash                               | 33.27            | 5  | Wen et al., 2011      |
| 8    | Guar gum–nano zinc oxide                              | 55.56            | 7  | Khan et al., 2013     |
| 9    | Wool  | 41.15            | 2  | Dakiky et al., 2002   |
| 10   | Olive cake  | 33.44            | 2  | „                     |
| 11   | Saw dust  | 15.82            | 2  | „                     |
| 12   | Almond  | 10.61            | 2  | „                     |
| 13   | Pine needles  | 7.08             | 2  | „                     |
| 14   | <i>Chrysophyllum albidum</i> (Sapotaceae) seed shells | 84.31            | 3  | Amuda et al., 2009    |
| 15   | Mosambi ( <i>Citrus limetta</i> ) peel                | 250              | 2  | Saha et al., 2013     |
| 16   | Modified rice husk                                    | 278              | 2  | El-Shafey, 2005       |
| 17   | Modified groundnut shell                              | 131              | 2  | This study            |

### 3.5. Comparison of Cr(VI) adsorption capacity of different adsorbents

The adsorption capacity of previously reported adsorbents for Cr(VI) were compared with the present results as shown in Table 3. It can be observed from the table that the maximum adsorption capacity ( $Q_{max}$ ) at solution pH 2.0 obtained in this study is higher (90 mg/g for UGS and 131 mg/g for MGS) when compared with the most recently reported adsorbents. This result indicates that the modified groundnut shell applied in this study is a better alternative to other low cost adsorbents. However, higher adsorption capacities of 250 and 278 mg/g were respectively reported for mosambi (*Citrus limetta*) peel (Saha et al., 2013) and modified rice husk (El-Shafey, 2005) at the same pH.

## 4. Conclusions

This paper presents unmodified and modified groundnut shells as low-cost adsorbent for effective removal of Cr(VI) ions from aqueous solutions. The removal efficiency was found to be dependent on the initial Cr(VI) ions concentration, temperature and contact time at optimum pH of 2. The isotherm data were analyzed by the Langmuir and Freundlich isotherms and the data fitted Freundlich model better than the Langmuir isotherm model. The maximum monolayer coverage adsorption capacity from the Langmuir isotherm model was obtained as 90 and 131 mg/g respectively for UGS and MGS at 28 °C. The kinetic data followed the pseudo-second-order kinetic model. The unmodified groundnut shells seem to work better in a solution with high concentration of Cr(VI) ions, but the modified groundnut shell was found to adsorbed Cr(VI) ions efficiently than that of the unmodified groundnut shell in most of the variable conditions.

## REFERENCES

Aksu Z. Determination of the equilibrium, kinetic and thermodynamic parameters of the batch biosorption of nickel(II) ions onto *Chlorella vulgaris*. *Process Biochem* 2002;38:89–99.

- Alfa-Sika MS, Liu F, Chen H. Optimization of key parameters for chromium(VI) removal from aqueous solutions using activated charcoal. *J Soil Sci Environ Manage* 2010;1: 55–62.
- Amuda OS, Adelowo FE, Ologunde MO. Kinetics and equilibrium studies of adsorption of chromium(VI) ion from industrial wastewater using *Chrysophyllum albidum* (Sapotaceae) seed shells. *Colloids Surf B Biointerfaces* 2009;68:184–92.
- Banat FA, Al-Bashir B, Al-Asheh S, Hayajneh O. Adsorption of phenol by bentonite. *Environ Pollution* 2000;107:391–8.
- Baruah AM, Karmakar A, Baruah JB. Ring opening reactions of pyromellitic dianhydride for the synthesis of first row transition dicarboxylate complexes. *Polyhedron* 2007;26: 4479–88.
- Cimino G, Passerini A, Toscano G. Removal of toxic cations and Cr(VI) from aqueous solution by hazelnut shell. *Water Res* 2000;34:2955–62.
- Dakiky M, Khamis M, Manassra A, Mer'eb M. Selective adsorption of chromium(VI) in industrial wastewater using low-cost abundantly available adsorbents. *Adv Environ Res* 2002;6: 533–40.
- Dehghani MH, Sanaei D, Ali I, Bhatnagar A. Removal of chromium(VI) from aqueous solution using treated waste newspaper as a low-cost adsorbent: kinetic modeling and isotherm studies. *J Mol Liquids* 2016;215:671–9.
- El-Shafey EI. Behaviour of reduction–sorption of chromium(VI) from an aqueous solution on a modified sorbent from rice husk. *Water Air Soil Pollut* 2005;163:81–102.
- Fourest E, Roux J-C. Heavy metal biosorption by fungal mycelial by-products: mechanisms and influence of pH. *Appl Microbiol Biotechnol* 1992;37:399–403.
- Freundlich HMF. Over the adsorption in solution. *J Phys Chem* 1906;57:385–471.
- Gardea-Torresday JL, Tiemann KJ, Armendariz V, Bess-Oberto L, Chianelli RR, Rios J, et al. Characterization of Cr(VI) binding and reduction to Cr(III) by the agricultural by products of *Avena monida* (Oat) biomass. *J Hazard Mater* 2000;80: 175–88.
- Garg VK, Gupta R, Kumar R, Gupta RK. Adsorption of chromium from aqueous solution on treated sawdust. *Bioresour Technol* 2004;92:79–81.
- Gupta SS, Bhattacharyya KG. Kinetics of adsorption of metal ions on inorganic materials: a review. *Adv Colloid Interf Sci* 2011;162:39–58.
- Han R, Zou W, Zhang J, Shi J, Yang J. Characterization of chaff and biosorption of copper and lead ions from aqueous solution. *Acta Sci Circums* 2006;26:32–9.

- Hasany SM, Saeed MM, Ahmed M, Radioanal J. Sorption and thermodynamic behavior of zinc(II)-thiocyanate complexes onto polyurethane foam from acidic solutions. Nucl Chem 2002;252:477-84.
- He Z, Yu J, Qi Y, Chi R. PMDA-modified biosorbents for enhancement adsorption of basic magenta. Environ Earth Sci 2013;70:635-42.
- Ho YS, McKay G. Pseudo-second order model for sorption processes. Process Biochem 1999;34:451-65.
- Kalaivani SS, Vidhyadevi T, Murugesan A, Thiruvengadaravi KV, Anuradha D, Sivanesan S, et al. The use of new modified poly(acrylamide) chelating resin with pendent benzothiazole groups containing donor atoms in the removal of heavy metal ions from aqueous solutions. Water Res Ind 2014;5:21-35.
- Kannan C, Muthuraja K, Devi MR. Hazardous dyes removal from aqueous solution over mesoporous aluminophosphate with textural porosity by adsorption. J Hazard Mater 2013;244-245:10-20.
- Karthikeyan T, Rajgopal S, Miranda LS. Chromium(VI) adsorption from aqueous solution by *Hevea Brasilensis* sawdust activated carbon. J Hazard Mater 2005;124:192-9.
- Khan T, Isa MH, Mustafa MRU, Yeek-Chia H, Baloo L, Abd Manana TSB, et al. Cr(VI) adsorption from aqueous solution by an agricultural waste based carbon. RSC Adv 2016;6:56365-74.
- Khan TA, Nazir M, Ali I, Kumar A. Removal of chromium(VI) from aqueous solution using guar gum-nano zinc oxide biocomposite adsorbent. Arabian J Chem 2013;In Press.
- Krishnani KK, Xiaoguang M, Christodoulatos C, Boddu VM. Biosorption mechanism of nine different heavy metals onto biomatrix from rice husk. J Hazard Mater 2008;153:1222-34.
- Langmuir I. The adsorption of gases on plane surfaces of glass, mica and platinum. J Am Chem Soc 1918;40:1361-403.
- Li Q, Zhai J, Zhang W, Wang M, Zhou J. Kinetic studies of adsorption of Pb(II), Cr(III) and Cu(II) from aqueous solution by sawdust and modified peanut husk. J Hazard Mater 2007;144:163-7.
- Mungasavalli DP, Viraraghavan T, Jin Y-C. Biosorption of chromium from aqueous solution by pretreated *Aspergillus niger*: batch and column studies. Colloids Surf A Physicochem Eng Asp 2007;301:214-23.
- Ofudje EA, Awotula AO, Oladipo GO, Williams OD. Detoxification of chromium(VI) ions in aqueous solution via adsorption by raw and activated Carbon prepared from sugarcane waste. Covenant J Phys Life Sci 2014;2:110-22.
- Rao M, Parwate AV, Bhole AG. Removal of Cr<sup>6+</sup> and Ni<sup>2+</sup> from aqueous solution using bagasse and fly ash. Waste Manage 2002;22:821-30.
- Saha R, Mukherjee K, Saha I, Ghosh A, Ghosh SK, Saha B. Removal of hexavalent chromium from water by adsorption on mosambi (*Citrus limetta*) peel. Res Chem Intermed 2013;39:2245-57.
- Sarin V, Pant KK. Removal of chromium from industrial waste by using eucalyptus bark. Bioresour Technol 2006;97:15-20.
- Sharma DC, Forster CF. The treatment of chromium wastewaters using the sorptive potential of leaf mould. Bioresour Technol 1994;49:31-40.
- Sharma PK, Ayub S, Tripathi CN. Isotherms describing physical adsorption of Cr(VI) from aqueous solution using various agricultural wastes as adsorbents. Cogent Eng 2016;3:1186857.
- Singh KK, Talat M, Hasan SH. Removal of lead from aqueous solutions by agricultural waste maize bran. Bioresour Technol 2006;97:2124-30.
- Sun G, Shi W. Sun flowers stalks as adsorbents for the removal of metal ions from wastewater. Ind Eng Chem Res 1998;37:1324-8.
- Tang Y, Chen L, Wei X, Yao Q, Li T. Removal of lead ions from aqueous solution by the dried aquatic plant, *Lemna perpusilla* Torr. J Hazard Mater 2013;244-245:603-12.
- Tella AC, Owalude SO, Ojekanmi CA, Oluwafemi OS. Synthesis of copper-isonicotinate metal-organic frameworks simply by mixing solid reactants and investigation of their adsorptive properties for the removal of the fluorescein dye. New J Chem 2014;38:4494-500.
- Umoren SA, Etim UJ, Israel AU. Adsorption of methylene blue from industrial effluent using poly(vinyl alcohol). J Mater Environ Sci 2013;4:75-86.
- Vidhyadevi T, Murugesan A, Kalaivani SS, Premkumar MP, Vinothkumar V, Ravikumar L, et al. Evaluation of equilibrium, kinetic, and thermodynamic parameters for adsorption of Cd<sup>2+</sup> ion and methyl red dye onto amorphous poly(azomethinethioamide) resin. Desalin Water Treat 2014;52:3477-88.
- Wang Q, Song J, Sui M. Characteristic of adsorption, desorption and oxidation of Cr(III) on birnessite. Energy Procedia 2011;5:1104-8.
- Wen Y, Tang Z, Chen Y, Gu Y. Adsorption of Cr(VI) from aqueous solutions using chitosan-coated fly ash composite as biosorbent. Chem Eng J 2011;175:110-16.
- Yan C, Li G, Xue P, Wei Q, Li Q. Competitive effect of Cu(II) and Zn(II) on the biosorption of lead(II) by *Myriophyllum spicatum*. J Hazard Mater 2010;179:721-8.
- Yu JX, Chi RA, Guo J, Zhang YF, Xu ZG, Xiao CQ. Desorption and photodegradation of methylene blue from modified sugarcane bagasse surface by acid TiO<sub>2</sub> hydrosol. Appl Surf Sci 2012;258:4085-90.
- Yu JX, Wang LY, Chi RA, Zhang YF, Xu ZG, Guo J. Adsorption of Pb<sup>2+</sup>, Cd<sup>2+</sup>, Cu<sup>2+</sup>, and Zn<sup>2+</sup> from aqueous solution by modified sugarcane bagasse. Res Chem Intermed 2015;41:1525-41.